Sodankylä Geophysical Observatory Publications (2003) 92:97–100

Triangulation of Auroral Red-Line Emission Heights

Brian J. Jackel, Fokke Creutzberg, Eric F. Donovan, and Leroy L. Cogger

Institute for Space Research, University of Calgary, Alberta, Canada

Keometrics, Ottawa, Ontario, Canada

Received: 6.12.2001 – Accepted: 16.5.2002

1 Introduction

Meaningful comparison of data from different platforms is often best accomplished if the data are viewed in a common coordinate system. This is often best facilitated by using geographic coordinates. As a consequence, the ability to take auroral emissions recorded by ground and satellite based instruments and infer the location of the source region is of fundamental importance to the scientific usefulness of optical auroral data. Mathematically, this is a simple coordinate transformation from azimuth and zenith angle to latitude and longitude. Additional information or assumptions about emission heights are usually also required. The only exceptions are for observations along the magnetic zenith, but such a configuration is difficult to achieve, and is not typical for most auroral imager or scanning photometer data. This study was originally motivated by the need to select an emission height appropriate for mapping auroral red-line (6300 Å) all-sky camera images.

Mapping in this way implicitly requires some drastic simplifications. Distributions of particle energy and pitch angle are complicated, and constantly changing. The resulting height profiles and horizontal variations in luminosity are definitely three-dimensional. In contrast, single wavelength measurements from one location give only a reduced two-dimensional view of the luminosity distribution.

Regardless, it is still frequently desirable to compare single site optical measurements with data from other instruments. Projecting to an assumed height is admittedly a crude approximation, but one that is required for certain kinds of spatial analysis such as studies of the polar cap boundary (Blanchard et al., 1997) or substorm dynamics (Friedrich et al., 2001). Of course, the limitations of simple mapping should always be kept in mind. Issues arising from errors in assumed emission height must be clearly understood, with a special effort made to minimize bias.

In this study we use photometers with overlapping fields of view to infer the height of 6300 Å auroral emissions. A simple triangulation technique is used to obtain heights from a 13 year data set. Most estimates fall in the 180-220 km height range, but there are a significant number of lower and higher values. Red-line heights are also found to be well correlated with standard spectral ratios.

Correspondence to: B.Jackel

2 Instruments and Data

The Canadian Auroral Network for the OPEN Program Unified Study (CANOPUS) array (Rostoker et al., 1995) consists of 13 autonomous stations located in Canada at sub-auroral, auroral, and polar cap latitudes. Four sites have multi-channel meridian scanning photometers (MSPs). These utilize eight-slot filter wheels spinning at 1200 RPM to provide effectively simultaneous measurements of signal and background emissions. A single cooled photomultiplier is used for all channels, so data is collected from each filter less than 1/8 of the total observing time.

In this paper we shall be concentrating primarily on the red-line (6300 Å) signal and background channels, with some limited use of the green-line (5577 Å) and $N_2^+ 1NG$ (4709 Å) channels. A stepping motor scans a mirror through 510 unevenly spaced positions from the northern to the southern horizon, aligned roughly along a magnetic meridian. Counts are corrected for detector-nonlinearity (pulse pileup) then grouped very coarsely to produce bins of equal latitudinal extent for assumed emission heights. E-region emissions (5577, 4709, 4861 Å) are averaged into 17 bins of 0.5° latitude at 110km, while the F-region emissions (6300 Å) are averaged into 16 bins of 1° latitude width at 230 km. Bin geometry is shown in figure 1, with the separation between beams exaggerated for clarity.

Although the MSP mirror stepping motor operates in 0.225° increments, the final data product has considerably lower angular resolution. A large number of measurements are made at different zenith angles, but these are averaged to produce a small number of bins at equally spaced latitudes. This is

done at the instrument level in order to lower telemetry requirements and simplify comparison of photometer data to other measurements. While obviously not ideal for studies which require high angular resolution, it is still sufficient for the relatively simple analysis methods used in this work.

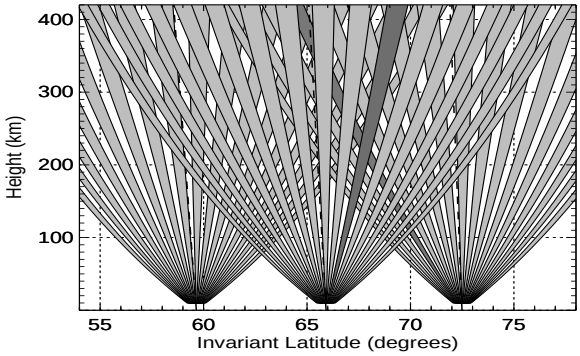

Fig. 1. Observing geometry for meridian scanning photometers at Pinawa, Gillam, and Rankin Inlet. Dashed lines indicate magnetic dipole field traced through each site.

Each meridian scan takes approximately 30 seconds; two of these are averaged to produce one multi-channel scan every minute. Background channels are subtracted using the appropriate constants for filter response to produce elevation scans of auroral emissions. The final processing stage is application of a Van Rhijn correction to E-region emission profiles, which is of course only strictly valid for homogenous emission layers at constant altitudes (Chamberlain, 1995). This will tend to produce an underestimate of the emission rate for narrow structures, but is necessary in order to usefully work with low elevation measurements. Meridian scans from the CANOPUS MSPs are typically projected on a latitude scale by assuming emission heights of 230 km for red-line emissions and 110 km for all other emissions. It is the appropriateness of the assumed red-line emission height which we will explore in this study.

The four MSPs are collectively referred to as the Meridian Photometer Array (MPA) and have been operating nearly continuously since 1988. When conditions are extremely active the auroral oval may be equatorward of the southern station at Pinawa. In the very early evening and late morning the oval may be poleward of the northern site at Rankin Inlet. For most conditions, however, the MPA provides excellent coverage of the nightside auroral oval. Data are collected from dusk to dawn (solar zenith angle greater than $96°$), which is a relatively short period during the summer but quite long at midwinter. Roughly half of the observations are of low quality due to partial or full cloud. Very little data is lost due to direct moonlight, although scattered moonlight may be a problem when haze is present, especially for weak auroral emissions. Finally, there are occasional instrumental failures and light pollution problems (primarily at Pinawa) which further reduce the fraction of useful data.

3 Analysis

CANOPUS MPA data from the period 1988 to 2001 are used in this study. During this time there are roughly 2 million overlapping scans from each pair of sites (Rankin/Gillam or Gillam/Pinawa), concentrated in the northern hemisphere wintertime. This number is reduced to less than 1 million after removing scans within an hour of lunar transit or with evidence of clouds at either site in each pair. An additional requirement is that the average apparent emission intensity in the overlap region be similar for both photometers. Large differences can occur if viewing conditions at one site are poor. While this has relatively little impact on triangulation heights, it will introduce errors into the calculation of spectroscopic ratios. During this part of the study we identified systematic differences (up to 50%) in the "absolute" intensities measured at different sites. We attempted to correct for this by using the central station (Gillam) as a standard. Intensities from the other sites were scaled to equalize the median values in the overlap regions. Finally, the peak red-line emission intensity in the overlap region is required to be at least 100 Rayleighs (R), and the red-line background channel less than 5 R/Å to ensure good signal to noise levels.

3.1 Correlation Height

Estimating emission heights by triangulation is not a new process, dating back to Störmer (1955). Perhaps the simplest method is to use only peak intensity (Boyd et al., 1971). Good angular resolution is required for this approach, which is sensitive to errors in the angular location of the intensity peak. Other techniques may be used to estimate height profiles in some cases (Romick and Belon, 1967). The logical extension would be application of tomography (Frey et al., 1998; Semeter et al., 1999) to maximize the amount of information that can be retrieved from any set of measurements.

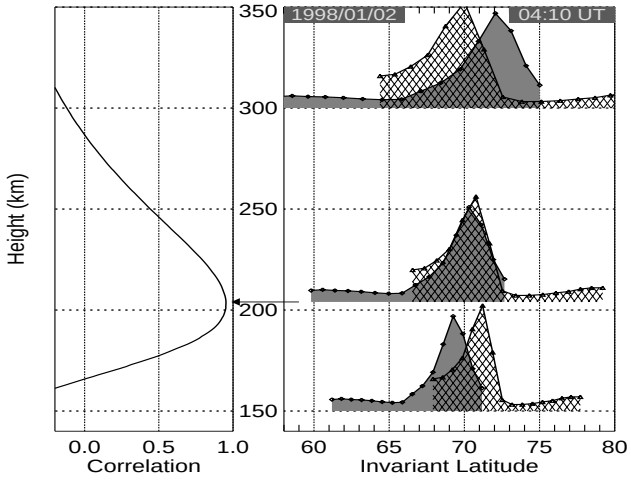

Fig. 2. Correlation variation with assumed height. Peak correlation ($r = 0.99$) occurs at a height of 215 kilometres.

Unfortunately, the CANOPUS MPA data are not well suited to tomographic analysis. Angular resolution is quite limited,

with a small number of overlapping measurements. Strong regularization (smoothing) or untestable assumptions about the luminosity distribution would be required to produce stable results. For this study we have simply used the correlation of two meridian scans projected onto a common invariant latitude grid at a range of assumed emission heights. This provides a correlation curve as a function of assumed altitude, with the peak correlation indicating the height where the best overlap occurs. Figure 2 contains an example of this process. When coherent structures are located in the overlap region, the correlation tends to vary smoothly with assumed height. This tendency has been used to accelerate the process of determining the height of peak correlation. A first pass with 5 km height resolution is used to roughly determine the peak, after which a second pass at 0.2km resolution to produce the final result.

Correlation height has the merits of being plausible, easily determined, and robust. One drawback is that the physical meaning is not obvious. We have done some modelling to study the behavior of correlation height for various emission structures and viewing geometries. For reasonable height and latitude profiles, and the site geometries used in this study, correlation height is roughly equivalent to the mean or centroid height. It is, however, possible that unusual conditions may produce a significant discrepancy between correlation and centroid height. Consequently, correlation height should be treated as a useful, but strictly empirical, quantity.

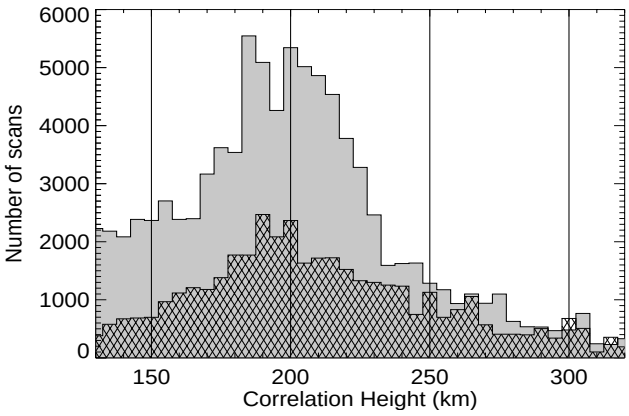

Fig. 3. Histograms of correlation heights in 5 km bins. Results for Rankin/Gillam are shown in light gray shading, with Gillam/Pinawa cross-hatched.

A correlation coefficient and estimated height may be obtained for any pair of scans, but the results will not always be physically meaningful. Heights shall be rejected if correlations are poor, or if the best peak correlation occurs when the two scans are barely overlapping. Results from all acceptable triangulations are shown in Figure 3. Both site pairs have fairly similar distributions, with a median value near 200km, despite the $\sim 5^\circ$ difference in magnetic latitude between the overlap regions. A significant number of peak correlations occur at low (<150km) altitudes. Many of these are simply due to the increased possibility of large correlations when there are fewer points in the overlap region. There are some events with distinct structures in 6300 Å that require low heights to produce reasonable correlations, however, the poor observing geometry at low altitudes makes these results somewhat questionable. Relatively few peak correlations occur at heights above 280 km. Given the extensive overlap at these heights, this is a reliable result.

3.2 Spectroscopic Ratios

It would be useful to have some indicator of what height(s) might be appropriate for any particular set of observations. Multiple wavelengths, if available, allow estimation of the characteristic energy of precipitating particles (Rees and Luckey, 1974; Strickland et al., 1989). Emission height profiles of 6300 Å can then be modelled as functions of this characteristic energy (Rees and Roble, 1986).

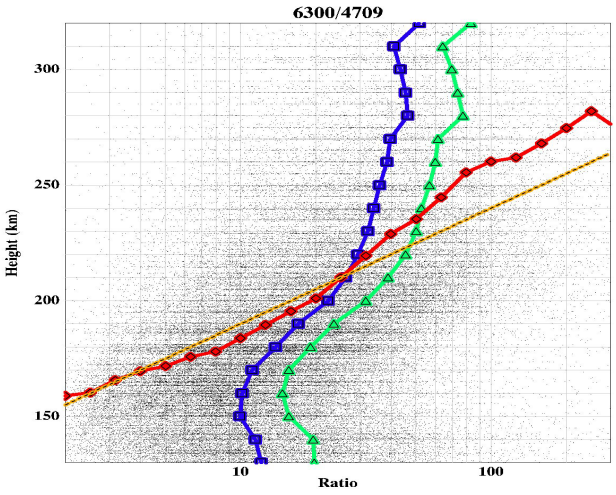

Fig. 4. Scatter plot of 6300Å / 4709Å versus correlation height. Red diamonds indicate dependence of height on spectral ratio, orange dashed line is model result of Rees and Roble (1986). See text for further details.

The ratio of 6300 Å / 4709 Å has been calculated for all cases that satisfied the requirements mentioned previously. As a further restriction, a peak value of at least 10R for 4709 Å is required in the overlap region in order to ensure reasonable signal levels. An approximate correction for airglow effects is accomplished by subtracting a value of 50R from all 6300 Å measurements (Steele and McEwan, 1990). Results are shown in Figure 4 for the approximately 70,000 cases which pass all tests. Binning by ratio produces a curve (red line with diamond symbols) that exhibits a nearly linear dependence on the logarithm of spectral ratio.

For comparison, the dashed orange line is the 6300 Å emission peak altitude predicted by the model of Rees and Roble (1986). Their results have been scaled assuming a constant ratio of $I4278/I4709 = 5$ (Jones and Gattinger, 1975) and extrapolated linearly outside the height range 180-240km. Agreement between model and observed trend of height as a function of emission ratio is surprisingly good. Slopes are identical, and the offset is consistent with a slightly asymmetric profile producing a centroid height (correlation height)

above the peak.

For an alternate perspective, it is interesting to consider height as the independent variable upon which spectral ratio depends. This interpretation has been explored by calculating the arithmetic (green triangles) and geometric (blue squares) means for each 5 km height bin. The linear trend is less pronounced, but still present between 160 and 280 km.

Figure 5 contains a similar display of $I6300/I5577$ versus H_c. This spectral ratio is often easier to measure, as green-line is much more intense than the N_2^+1NG emission at 4709Å. Disadvantages include uncertainties in removing the background airglow contribution, and the weaker theoretical basis for using this ratio as an estimator of characteristic energy. As with figure 4, there is a clear linear trend in triangulation height with log ratio, and a less pronounced dependence of spectral ratio on height.

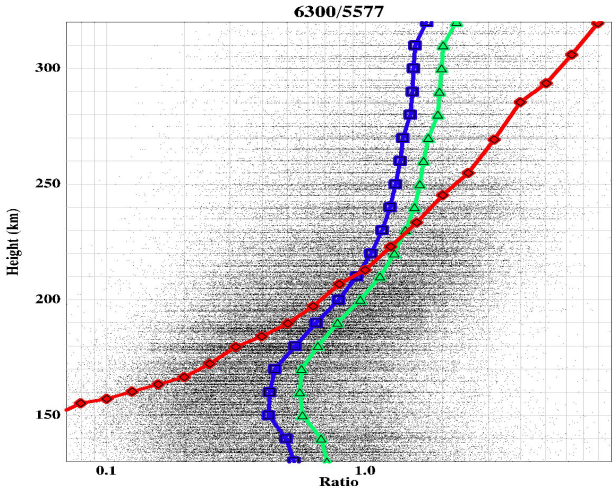

Fig. 5. Scatter plot of 6300Å / 5577Å versus correlation height. Symbols are the same as in figure 4

4 Discussion

The primary goal of this study was to test the validity of using 230 km as an assumed emission height for 6300 Å aurora. The distribution of heights obtained from triangulation (Figure 3) indicates that 200 km may be a more reasonable value. However, there is also a great deal of variation, and for a particular situation the "correct" value might lie between 180 to 220 km.

There is clearly a strong statistical relationship between correlation height and spectroscopic ratios. Equally clearly, there is also a great deal of scatter. Some fraction of this will be due to errors in estimating the correlation height. A larger source of variability probably arises by errors in determining spectroscopic ratios from intensity measurements. Differences in airglow levels and effects due to haze and cloud are difficult to identify, but may introduce significant amounts of scatter. Finally, the basic concept of a single spectroscopic ratio as an indicator of precipitation energy (and hence height) is overly simplistic. Changes in atmospheric parameters such as atomic oxygen or electron density may significantly alter emission rates (Strickland et al., 1989). Having said this, it should noted that other studies (Vondrak and Sears, 1978; Mende et al., 1984) have found good agreement between simple ratios and characteristic energy determined by other methods.

Acknowledgements. B.J. was partially supported by funds from the Canadian Natural Sciences and Engineering Research Council and the Canadian Space Agency. The CANOPUS array is maintained and operated by the Canadian Space Agency.

References

Blanchard, G., Lyons, L., and Samson, J., Accuracy of using 6300 Å auroral emission to identify the magnetic separatrix on the nightside of Earth, *J. Geophys. Res.*, *102*, 9697–9703, 1997.

Boyd, J., Belon, A., and Romick, G., Latitude and time variations in precipitated electron energy inferred from measurements of auroral heights, *J. Geophys. Res.*, *76*, 7694–7700, 1971.

Chamberlain, J. W., *Physics of the aurora and airglow*, American Geophysical Union, Washinton, D.C., reprint edn., 1995.

Frey, H. U., Frey, S., Lanchester, B. S., and Kosch, M., Optical tomography of the aurora and EISCAT, *Ann. Geophysicae*, *16*, 1332–1342, 1998.

Friedrich, E., Samson, J., Voronkov, I., and Rostoker, G., Dynamics of the substorm expansive phase, *J. Geophys. Res.*, *106*, 13,145–13,163, 2001.

Jones, A. V. and Gattinger, R., Quantitative spectroscopy of the aurora. III. The spectrum of medium intensity aurora between 3100 Å and 4700 Å, *Can. J. Phys.*, *53*, 1806–1813, 1975.

Mende, S., Eather, R., Rees, M., Vondrak, R., and Robinson, R., Optical mapping of ionospheric conductance, *J. Geophys. Res.*, *89*, 1755–1763, 1984.

Rees, M. and Luckey, D., Auroral electron energy derived from ratio of spectroscopic emissions 1. model computations, *J. Geophys. Res.*, *79*, 5181–5186, 1974.

Rees, M. and Roble, R., Excitation of $O(^1D)$ atoms in aurorae and emission of the [0I] 6300-Å line, *Can. J. Phys.*, *64*, 1608–1613, 1986.

Romick, G. and Belon, A., The spatial variation of auroral luminosity- II Determination of volume emission rate profiles, *Planet. Space Sci.*, *15*, 1695–1716, 1967.

Rostoker, G., Samson, J., Creutzberg, F., Hughes, T., McDiarmid, D., McNamara, A., Jones, A. V., Wallis, D., and Cogger, L., CANOPUS-a ground based instrument array for remote sensing the high latitude ionosphere during the ISTP/CGS program, *Space Sci. Rev.*, *71*, 743–760, 1995.

Semeter, J., Mendillo, M., and Baumgardner, J., Multispectral tomographic imaging of the midlatitude aurora, *J. Geophys. Res.*, *104*, 24,565–24,585, 1999.

Steele, D. and McEwan, D., Electron auroral excitation efficiencies and intensity ratios, *J. Geophys. Res.*, *95*, 10,321–10,336, 1990.

Störmer, C., *The polar aurora*, Clarendon Press, Oxford, 1955.

Strickland, D., Meier, R., Hecht, J., and Christensen, A., Deducing composition and incident electron spectra from ground-based auroral optical measurements: theory and model results, *J. Geophys. Res.*, *94*, 13,527–13,539, 1989.

Vondrak, R. R. and Sears, R. D., Comparison of incoherent scatter radar and photometric measurements of the energy distribution of auroral electrons, *J. Geophys. Res.*, *83*, 1665–1667, 1978.